Probing the Coupling of Charge-Transfer Processes Across Liquid/Liquid Interfaces by the Scanning Electrochemical Microscope

Yoram Selzer and Daniel Mandler*

Department of Inorganic and Analytical Chemistry, The Hebrew University of Jerusalem, Jerusalem 91904, Israel

Received: October 27, 1999; In Final Form: February 10, 2000

The feedback mode of the scanning electrochemical microscope (SECM) is used to induce and measure charge-transfer coupling (CTC) between two ion-transfer (IT) processes across liquid/liquid interfaces. Results are interpreted using a general model for coupling processes under steady-state conditions that is also applicable to other modes of coupling such as IT−ET and ET−ET (ET = electron transfer). The measured feedback curves demonstrate the effect of mass-transfer limitations in these processes on the potential across the interface, shedding new light on the dynamics of bioenergetics and phase-transfer catalysis systems as well as on previous SECM studies of liquid/liquid interfaces.

Introduction

By charge-transfer coupling (CTC) we define the mutual effect that two (or more) charge-transfer processes have, when they take place simultaneously across an interface. More specifically, we are interested in systems where the potential across the interface is not controlled by an extraneous source but by the distribution of the charge carriers across the interface. The mutual effect is manifested by the dependence of the kinetics of the various charge-transfer processes on the resulting potential across the interface.

CTC processes play a key role in many biological systems[1] (such as the chemiosmotic proton circuit and electroneutral symport and antiport processes) as well as in much simpler systems, such as phase-transfer catalysis.[2−4] This paper concerns CTC across liquid/liquid interfaces. Since these interfaces had been proposed in the past as simple models for biological membranes,[5,6] our discussion and in particular our approach might be useful for treating charge transfer in biological systems. Although significant progress has been achieved in understanding these interfaces[7] and the kinetics of charge transfer across them,[8,9] the understanding of charge-transfer coupling mechanisms is still rather poor.

Charge can be transferred across liquid/liquid interfaces by means of ion transfer (IT) or electron transfer (ET). Historically, charge-transfer studies initiated with the so-called conventional methods, i.e., interface polarization using appropriate reference electrodes on both sides of the interface.[9] These methods suffer from several experimental drawbacks: lack of ability to discriminate between IT and ET, distortions due to charging current, *iR*-drop in nonaqueous solutions, and limited potential window dictated by the nature of the electrolyte. The conventional methods also lack the ability to investigate CTC processes that can be either ET−IT or IT−IT.

The introduction of the scanning electrochemical microscope (SECM) as an experimental tool for investigating liquid/liquid interfaces circumvented some of the above experimental problems.[10] The SECM has been used to study ET[10−14] as well as IT processes.[15,16] The main objective of these studies was to elucidate the dependence of various charge-transfer processes on the potential across the interface. The potential was controlled by using potential-determining ions. In these experiments charge was forced to cross a liquid/liquid interface not by polarizing it but as a result of generating an oxidizing/reducing agent near the interface (in the case of ET) or upon inducing a change in ion distribution across the interface (in the case of IT). As a result the steady-state charge-transfer processes under investigation were coupled to compensating IT processes that maintain electroneutrality. Because potential-determining ions in these studies also serve as charge-compensating ions, their concentration must be sufficiently high to ensure that compensating processes will not become the rate-limiting steps.

Previous studies avoided the complex situation involving low concentrations of compensating ions. We continue from this point and explore the effect of low concentration of potential-determining/compensating ions on the kinetics of charge transfer. Experiments under such conditions focus on the effect of mass-transfer limitations of the compensating ions on the overall processes.

Our model system was first studied by Mirkin et al.[17] using the SECM and is schematically depicted in Figure 1. It is based on the process of facilitated K^+ transfer by dibenzo-18-crown-6 (DB18C6) from water into 1,2-dichloroethane (DCE), a process which has been investigated extensively in the past:[8,18−22]

$$K^+(w) + DB18C6(DCE) \leftrightarrow [K^+DB18C6](DCE) \quad (1)$$

In essence, a glass-pulled micropipet consisting of K^+ ions in an aqueous phase was polarized vs a reference electrode located in DCE that also contained the K^+-complexing agent DB18C6. The potential inside the micropipet was set to a positive value for which the extraction of K^+ was diffusion controlled. DB18C6 carrying the K^+ ion diffuses away from the micropipet to the lower DCE/W (W = water) interface. By releasing K^+ ion across that interface into the aqueous phase, DB18C6 is regenerated to its neutral form, and by diffusing back to the micropipet establishes the feedback effect. The kinetics of K^+ transfer across the lower interface depends on the potential $\Delta_o^w\varphi$, which in turn depends on the ratio of concentrations of a potential-determining ion (in our case tetrabutylammonium, TBA^+) in the two liquid phases according to the Nernst−

10.1021/jp993808i CCC: $19.00
Published on Web 04/29/2000

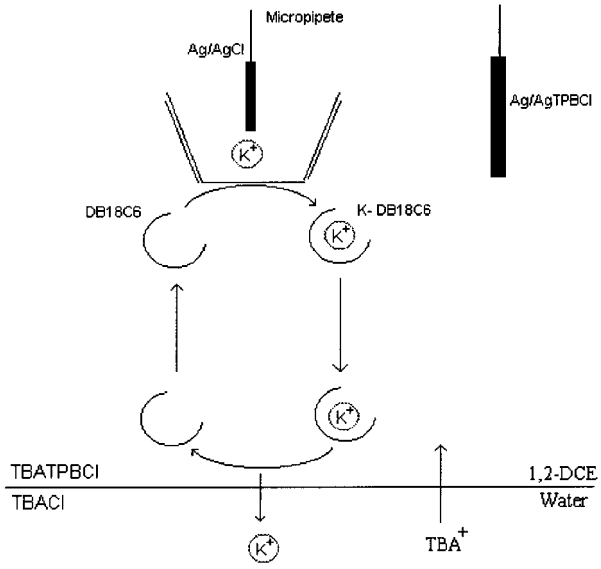

Figure 1. Schematic representation of the experimental setup: a SECM micropipet tip in close proximity to a DCE/W interface. The feedback loop is established by the crown ether: DB18C6. K^+ is extracted out of the micropipet by a mechanism of interfacial complexation (eq 1) and is released into the bottom aqueous phase upon interfacial dissociation. TBA^+ ion transfer maintains electroneutrality in both phases.

Donnan equation:[7]

$$\Delta_o^w\varphi = \Delta_o^w\varphi^0_{TBA^+} + \frac{RT}{zF}\ln\frac{C^o_{TBA^+}}{C^w_{TBA^+}} \qquad (2)$$

where $\Delta_o^w\varphi^0_{TBA^+}$ is the standard transfer potential of TBA^+, $C^o_{TBA^+}$ and $C^o_{TBA^+}$ are its concentrations in the organic and aqueous phases, respectively, and the rest of the variables have their usual meaning. It is worth mentioning that on the basis of thermodynamic data it is evident that both hydrophilic ions, i.e., K^+ and Cl^-, are not likely to be distributed between the two phases but rather stay in the aqueous phase only.

The transfer of K^+ into the aqueous phase should be compensated by another charge-transfer process. As will be explained later, all the ions of this system were carefully selected to ensure that only TBA^+ could be that compensating ion. This duality in the role of TBA^+ in this system (potential-determining as well as charge-compensating ion) is the essence of this paper. It enables us to demonstrate how the SECM can probe the dynamics of charge-transfer coupling, focusing on the effect of mass-transfer limitations on this process. As will be shown later, in this unique case the potential across the interface shifts locally from its initial equilibrium value as the mass transport characteristics of the ions involved in the system are changed. Under SECM conditions the mass transfer of the ions depends on the distance of the micropipet from the DCE/W interface.

Experimental Section

The SECM system was described previously.[23] A two-electrode setup was employed: The micropipet (typically with an orifice radius in the range of 10−25 μm) was back-filled with a 100 mM KCl solution, to inhibit any mass-transfer effects inside the pipet. A pre-anodized 0.1 mm Ag wire was inserted into the pipet from the back. The outer walls of all the pipets that were used were silanized, as was previously suggested.[24] This treatment ensured that the pipets would exhibit a disklike electrochemical behavior. A 0.25 mm Ag wire coated with AgTPBCl served as an organic reference electrode (TPBCl = tetrakis[4-chlorophenyl]borate). In all liquid/liquid experiments the concentrations of (TBA)(TPBCl) (in DCE) and TBACl (in water) were 5 mM. The concentration of DB18C6 varied in the range of 0.5−5 mM.

The SECM experiments were conducted using the feedback mode. The potential on the micropipet was set to 420 mV to drive the facilitated extraction of K^+ into the organic phase in a diffusion-controlled manner. Using the high-resolution movement capabilities of the SECM, the micropipet was made to approach the lower interface between DCE and water while monitoring its current. The necessary experimental configuration which enables this unique configuration of the heavy DCE phase on top of water has been described previously.[17]

Theory

The Model. When charge crosses a liquid/liquid interface with a certain rate under steady-state conditions, the need for electroneutrality dictates a compensating charge transfer with the same rate. As a result the interface attains a mixed potential, $\Delta_o^w\varphi_{mix}$, for which the rates, and obviously also the currents, of both processes are equal. Each of the coupled charge-transfer processes has its own characteristic i-$\Delta_o^w\varphi$ curve. As soon as the potential of the interface is $\Delta_o^w\varphi_{mix}$, the current flowing in one direction must equal the opposite flow. The current is then defined as i_{mix}. This approach is commonly used for modeling the corrosion phenomenon where an ET process is coupled to IT from the solid phase to the liquid phase. In the latter case, a mixed potential is attained at the interface in which the anodic current (which causes the metal to corrode) equals the cathodic current (which is usually due to oxygen reduction). To the best of our knowledge, this sort of reasoning has been suggested previously only once to analyze CTC processes, however without any real time experimental ability to measure its dynamics.[4]

The formulation of the model, which is described here, is exemplified by coupling two reversible reactions. As will be justified later, the two IT processes in our system are indeed reversible under all mass-transfer conditions. Obviously, the model can be constructed to be more general, applicable to any IT−IT regardless of their reversibility. The necessary changes should be obvious.

Applying the Model to SECM Problems. This model was applied previously by us for analyzing heterogeneous redox catalysis on metal surfaces by the SECM.[23] We regarded that system as an ET−ET coupling process. Several characteristics of that system simplified the application of the model: The metal surface ensured that the interface would be an equipotential surface. Therefore, although the flux to the metal surface was not uniform, the high conductivity of the metal established a uniform potential. As a result, the area of the interface where coupling took place was essentially the area of the entire metal surface, which did not change during the feedback experiment. Hence, single values of $\Delta_o^w\varphi_{mix}$ and i_{mix} characterized the entire interface.

In the case of a liquid/liquid interface, under SECM conditions, the situation is substantially more complicated. The nonuniform flux of the ion−ionophore complex (K^+DB18C6) as well as that of the TBA^+ ion to the DCE/W interface establishes a steady-state distribution of $\Delta_o^w\varphi_{mix}$ and i_{mix}. Because the configuration of the micropipet in close proximity to the interface has a cylindrical symmetry, the potential distribution must have a circular symmetry. To find this distribution, it is necessary to construct analytical approxima-

tions for the different $i-\Delta_o^w\varphi$ curves at each point on the interface.[23] These curves in turn are based on the ability to solve the two-dimensional diffusion−migration equations for the different ions using the boundary conditions of charge-transfer kinetics defined by $\Delta_o^w\varphi_{mix}$. Therefore, the overall solving process involves a complex iterative procedure that is extremely difficult to implement and is beyond the scope of this paper. In addition, the active area on the interface through which the coupling process takes place depends on the distance of the micropipet from the interface.[25] In SECM terminology, the active area is simply the area on the substrate where the feedback process takes place. In our case it is a virtual area on the lower interface where the ion−ionophore complex is dissociated (releasing K^+ across the interface), regenerating DB18C6 in its neutral form. In previous publications[12−15] it was argued that compensating IT processes occur all over the interface. We argue that these processes (represented here by the IT of TBA^+) take place only throughout the active area. The reason for this argument is the following: TBA^+ ions are initially in equilibrium. This means that there is no net flux of TBA^+ across the interface. To establish a flux, the equilibrium potential must be perturbed. In our system the transfer of K^+ induces the perturbation. The closer the micropipet is to the DCE/W interface, the more significant is the perturbation. Beyond the diffusion layer of the micropipet there is no equilibrium perturbation; i.e., there is no IT of TBA^+. From the point of view of TBA^+, the circular (active) area on the interface, through which K^+ is transferred, acts like a microelectrode with a circular distribution of potential governed by the concentration ratio of K^+ on both sides of the interface.

To understand the general behavior of the system and to make quantitative predictions in a simple manner, we apply the model in two extreme cases, where the distribution of mixed potential across the interface, $\Delta_o^w\varphi_{mix}$, is almost uniform. The first case applies when the micropipet is brought very close to the DCE/W interface so that the flux of the ion−ionophore complex to the interface is uniform.[26,27] On the other hand, holding the micropipet far enough from the DCE/W interface makes the flux to that interface sufficiently small to be regarded as uniform.

IT of TBA^+. TBA^+ serves as the potential-determining ion in our system. The equilibrium potential is described by the Nernst−Donnan equation. The system resembles a common redox system where the two redox states are initially present. This similarity suggests that the i-$\Delta_o^w\varphi$ curve for TBA^+ should be constructed starting with the following equation:[28]

$$\Delta_o^w\varphi = \Delta_o^w\varphi^0_{TBA^+} + \frac{RT}{zF}\ln\frac{D^w_{TBA^+}}{D^o_{TBA^+}} + \frac{RT}{zF}\ln\left[\frac{i_{TBA^+} - i^{l,o}_{TBA^+}}{i^{l,w}_{TBA^+} - i_{TBA^+}}\right] \quad (3)$$

where

$$i^{l,o}_{TBA^+} = 4nFD^o_{TBA^+}C^o_{TBA^+}a\gamma \quad (4)$$

and

$$i^{l,w}_{TBA^+} = 4nFD^w_{TBA^+}C^w_{TBA^+}a\gamma \quad (5)$$

are the diffusion-controlled currents of TBA^+ to the active area on the DCE/W interface from the organic and aqueous phases, respectively. $D^o_{TBA^+}$ and $D^w_{TBA^+}$are the diffusion coefficients of TBA^+ in the organic and aqueous phases, $C^o_{TBA^+}$ and $C^w_{TBA^+}$ are the bulk concentrations of TBA^+ in these phases, and γ is the ratio between the radius of the circular active area on the DCE/W interface and the orifice radius, a, of the micropipet.

By defining $\Delta_o^w\varphi^{0'}_{TBA^+}$ and θ_{TBA^+} as

$$\Delta_o^w\varphi^{o'}_{TBA^+} = \Delta_o^w\varphi^0_{TBA^+} + \frac{RT}{zF}\ln\frac{D^w_{TBA^+}}{D^o_{TBA^+}} \quad (6)$$

and

$$\theta_{TBA^+} = \exp\left[\frac{zF}{RT}(\Delta_o^w\varphi - \Delta_o^w\varphi^{0'}_{TBA^+})\right] \quad (7)$$

We can rearrange eq 3 to give

$$i_{TBA^+} = \frac{\theta_{TBA^+}i^{l,w}{}_{TBA^+} + i^{l,o}{}_{TBA^+}}{1 + \theta_{TBA^+}} \quad (8)$$

which is the $i-\Delta^w{}_o\varphi$ for TBA^+.

IT of K^+. The transfer of potassium ion from water into DCE facilitated by DB18C6 has been extensively investigated in the past.[18−22] To simplify those studies, the concentration of the potassium ion in the aqueous phase was much higher than that of DB18C6 in the organic phase, thus eliminating any contribution of mass-transfer limitations inside the aqueous phase on the measured voltammograms. Under steady-state conditions the voltammogram for K^+ transfer is given by[20]

$$\Delta_o^w\varphi = \Delta_o^w\varphi^0_{K^+} + \frac{RT}{zF}\ln\left(\frac{D^o_{DB18C6}}{D^o_{K^+DB18C6}}\right) - \frac{RT}{zF}\ln(K^0C_{K^+}) + \frac{RT}{zF}\ln\left(\frac{i}{i_l - i}\right) \quad (9)$$

where K^0 is the association constant of K^+DB18C6 in the organic phase, D_{DB18C6} and $D_{K^+DB18C6}$ are the diffusion coefficients of the ionophore and the ion−ionophore complex, respectively, and i_l is the diffusion-controlled current of DB18C6 to the interface. In our system things are slightly more complicated. The process at the DCE/W interface is not exactly the reverse process of that at the micropipet. As the lower aqueous phase does not contain any K^+ initially, we cannot ignore the influence of K^+ diffusion away from the interface into the bulk of that phase. Taking the latter into account leads to the following voltammogram (see the Appendix): Here, i_l is

$$\Delta_o^w\varphi = \Delta_o^w\varphi^0_{K^+} + \frac{RT}{zF}\ln K^0 + \frac{RT}{zF}\ln(4nFD^w{}_{K^+}\gamma a) - \frac{RT}{zF}\ln\left(\frac{i^2}{i_l - i}\right) \quad (10)$$

the diffusion-controlled current of the ion−ionophore complex to the interface. An unusual voltammogram like this always results when mass-transfer effects in both phases are taken into account.[29] By defining θ_{K^+} as

$$\theta_{K^+} = \exp\left\{\frac{-zF}{RT}\left[\Delta_o^w\varphi - \left(\Delta^w{}_o\theta^0{}_{K^+} + \frac{RT}{zF}\ln K^0 + \frac{RT}{zF}\ln(4nFD_{K^+}a)\right)\right]\right\} \quad (11)$$

the $i-\Delta_o^w\varphi$ curve for the IT of K^+ is the positive root of the quadratic equation

$$i^2 + \theta_{K^+}i - \theta_{K^+}i_l = 0 \quad (12)$$

Normalization. The above currents are normalized relative to i_{DB18C6}^{diff}, the diffusion-controlled current of DB18C6 to the micropipet ($4nFD^{o}_{DB18C6}C^{o}_{DB18C6}a$). It is quite easy to see that in the case of TBA^+ the normalized current is

$$I_{TBA^+} = \frac{i_{TBA^+}}{i_{DB18C6}^{diff}} = \frac{\theta_{TBA^+}\dfrac{D^{w}_{TBA^+}C^{w}_{TBA^+}}{D^{o}_{DB18C6}C^{o}_{DB18C6}} - \dfrac{D^{o}_{TBA^+}C^{o}_{TBA^+}}{D^{o}_{DB18C6}C^{o}_{DB18C6}}}{1+\theta_{TBA^+}} \quad (13)$$

where all the concentrations are bulk values.

For K^+, normalization of eq 12 gives

$$I_{K^+}{}^2 + \theta'_{K^+}I_{K^+} - \theta'_{K^+}I^{diff}_{K^+} = 0 \quad (14)$$

where $I^{diff}_{K^+}$ is the normalized diffusion-controlled current of the ion−ionophore complex to the DCE/W interface, and θ'_{K^+} is now defined as

$$\theta'_{K^+} = \exp\left[\frac{-zF}{RT}\left[\Delta^{w}_{o}\varphi - \left(\Delta^{w}_{o}\varphi^{0}_{K^+} + \frac{RT}{zF}\ln K^0 + \frac{RT}{zF}\ln C^{*}_{DB18C6} + \frac{RT}{zF}\ln\gamma\right)\right]\right] \quad (15)$$

assuming $D^{o}_{DB18C6} = D^{o}_{K^+DB18C6}$.

Simulations. Diffusion-controlled currents at the micropipet, at the lower DCE/W interface, and at the radius of the active area were simulated. Simulations were carried out using the ADI finite difference method that has been demonstrated to be extremely suitable for SECM problems.[30] All simulations considered the fact that the insulator around a micropipet is extremely small, making it necessary to take diffusion "behind" the micropipet under consideration. See ref 31 for more details.

Results and Discussion

Micropipet Characterization. Small liquid/liquid interfaces located at the end of micropipets were first suggested and used by Girault.[19,32] The measured currents at these micropipets turned out to be higher than the currents expected at disk-shaped ultramicroelectrodes, suggesting that the interface at the end of micropipets is probably hemispherical or subhemispherical.[32] Mirkin[24] proved that this discrepancy is probably due to partial wetting of the outer walls of micropipets, close to their orifice, by the inner aqueous solution. Obtaining disk-shape behavior with micropipets is possible by careful silanization of their outer walls.[24] This procedure enabled Mirkin to use micropipets as well-characterized tips for SECM.[15] Accordingly, all the pipets in this study were silanized prior to their use, and their geometry was verified by voltammetry. A typical steady-state voltammogram of K^+ transfer from water into DCE is depicted in Figure 2. The diffusion-controlled current is higher by 28% than the expected current on a disk-shaped microelectrode ($4nFDCa$). This result is in perfect agreement with theoretical calculations, and is due to the thin insulator around the electrode.[15,31]

Choice of Potential-Determining Compensating Ion. To simplify the discussion, it is extremely crucial to construct a system in which only one specific ion participates in the compensating process. As this ion should also be potential-determining, we cannot avoid its presence in both phases. Obviously, it must not interfere with K^+ extraction out of the micropipet.

Previous studies of facilitated K^+ transfer across DCE/W interfaces[19,21,22] used (TBA)(TPBCl) as the electrolyte in the organic phase. Comparing both ions comprising this electrolyte

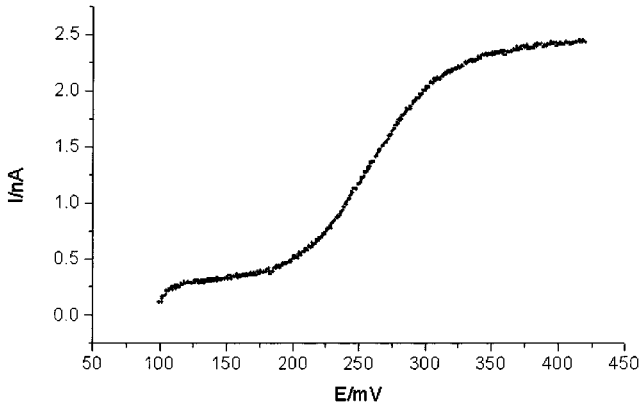

Figure 2. A steady-state voltammogram of facilitated K^+ transfer for a micropipet with an internal radius of 17.5 μm and an outer radius of 18.5 μm. K^+ concentration 100 mM, DB18C6 concentration 0.5 mM, (TBA)(TPBCl) concentration 5mM, and scan rate 25 mV/s.

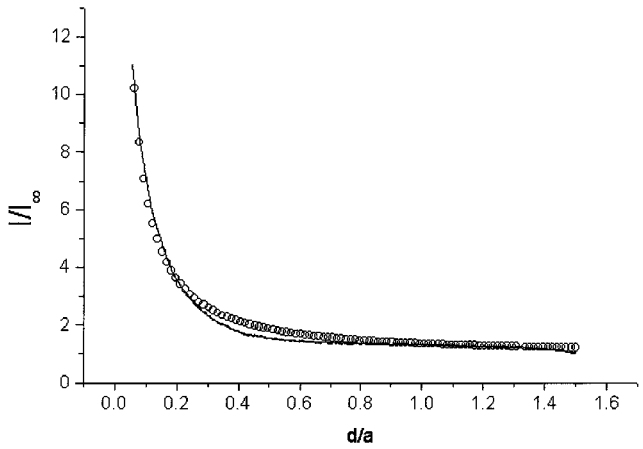

Figure 3. Experimental feedback curve (—) vs a theoretical curve (○) calculated for a diffusion-controlled process. DB18C6 concentration 0.5 mM. The concentration of TBA^+ in both phases was 5 mM, setting the potential across the DCE/W interface to be $\Delta^{w}_{o}\varphi^{0}_{TBA^+}$. The potential on the micropipet was typically 420 mV.

suggests that TBA^+ is superior for our purposes, on the basis of the following reasoning: The potential window in Figure 2 is limited on one side (ca. $E = 0$ V) by TBA^+ transfer from the organic phase into the micropipet, and on the other side by $TPBCl^-$ transfer in the same direction. The process at the DCE/W interface below the micropipet is the reverse of the one that is depicted in Figure 2, i.e., K^+ stripping into the lower aqueous phase. Throughout the potentials of this process, ITs of TBA^+ and $TPBCl^-$ are allowed only from the aqueous phase into the organic phase. This rules out the possibility of $TPBCl^-$ transfer, because to maintain electroneutrality this anion should cross the interface in the same direction of K^+. Hence, TBA^+ is left as the trivial choice for our needs. TBA^+ also has an additional important advantage that simplifies the discussion. Namely, the reported[9] standard rate constant for TBA^+ transfer is sufficiently high to ensure reversibility across the lower interface under the mass-transfer characteristics of our system.

Preliminary Assessment of the System. Figure 3 shows that a reasonable agreement is obtained between the theoretical and experimental positive (diffusion-controlled) feedback currents. These conditions are achieved by setting the potential across the DCE/W interface on $\Delta^{w}_{o}\theta^{0}_{TBA^+}$ (using a concentration ratio of $C^{o}_{TBA^+}/C^{w}_{TBA^+} = 1$). Since the theoretical curve was calculated for a disk ultramicroelectrode, this serves as an additional proof for the disk-type geometry of the micropipet. The diffusion-controlled feedback observed at the above potential

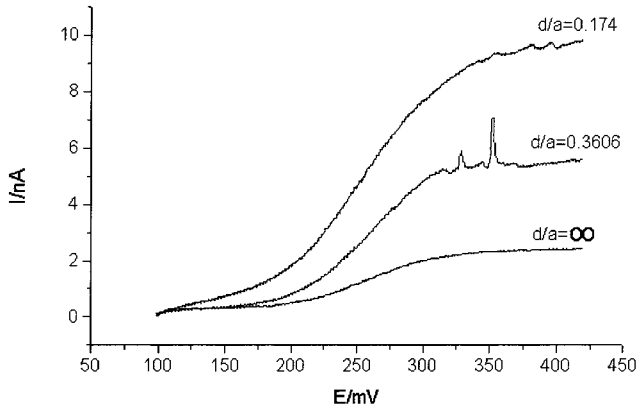

Figure 4. Steady-state voltammograms at a micropipet with an internal radius of 17 μm measured at different distances from the DCE/W interface. The experimental conditions as in Figure 3, ensuring diffusion-controlled mass-transfer enhancement of DB18C6 to the micropipet. The normalized distances are depicted on top of the curves.

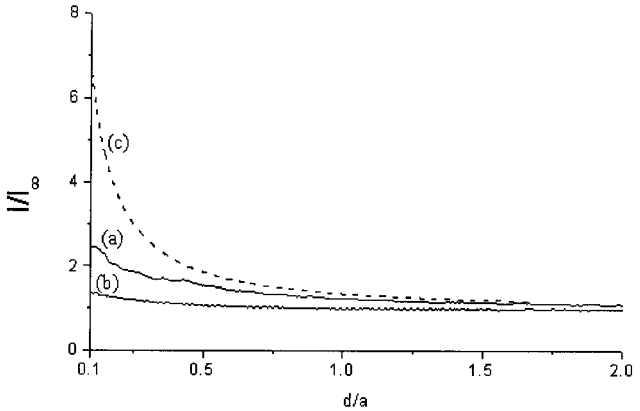

Figure 5. Feedback curves under IT limitations. The initial TBA^+ concentration in both phases was 5 mM. The DB18C6 concentration was (a) 2.5 mM, (b) 5 mM, and (c) 0.5mM (see Figure 3). The K^+ concentration inside the micropipet was 100 mM.

is expected as TBA^+ transfer occurs at potentials in which K^+ stripping is diffusion-controlled. The standard rate constant for K^+ transfer has only recently been reported to be on the order of 1 cm/s,[21] suggesting that under our mass-transfer conditions K^+ should behave reversibly. To test this assumption, a set of voltammograms on the micropipet were recorded at different distances from the DCE/W interface, i.e., under varying mass-transfer conditions. The interface was constantly poised at $\Delta_o^w\theta^0_{TBA^+}$. Several resulting steady-state voltammograms are shown in Figure 4. All turned out to be essentially reversible as analyzed following the method of Mirkin and Bard ($\Delta E_{1/4}$, $\Delta E_{3/4} \approx 30$ mV).[33]

Coupling under Mass-Transfer Limitations. The feedback in Figure 3 was measured under a 10-fold excess of TBA^+ concentration over that of DB18C6. As described before, the initial equilibrium potential across the DCE/W interface was set to $\Delta_o^w\theta^0_{TBA^+}$. The fact that the regeneration of free DB18C6 remained diffusion-controlled even at very short distances does not necessarily imply that the potential across the interface remained at this fixed value throughout the approach. It rather suggests that, under an excess of TBA^+, the interfacial potential did not attain values that were outside the potential window, in which the feedback is diffusion-controlled.

The potential is expected to shift because of IT−IT coupling. That is, TBA^+ crosses the interface, to DCE, to electroneutralize the transfer of positive charge, i.e., K^+ going in the opposite direction. This alters the concentration of TBA^+ on both sides of the interface, establishing a new potential, $\Delta_o^w\theta$, according to the Nernst−Donnan equation (eq 2). As long as the concentration of TBA^+ is in excess, the change of potential is only minor, leading to a diffusion-controlled feedback. This is demonstrated more quantitatively in Figure 6a,b. The i-$\Delta_o^w\varphi$ curves of the two coupled IT processes at the DCE/W interface are shown for normalized distances of $L = 2$ and $L = 0.1$, respectively. As the distance between the micropipet and the DCE/W interface decreases, the mass transfer of the ion−ionophore complex is enhanced, resulting in a higher curve for K^+ transfer. At the same time, the change in the TBA^+ curve is only minor because of its excess. The small change that can be seen results from a decrease in the active area on the interface as a function of L. It is evident that even at short distances the potential of intersection, $\Delta_o^w\varphi_{mix}$, does not change appreciably from the initial equilibrium value ($\Delta_o^w\varphi^0_{TBA^+}$) and it continues to remain in the plateau area of the K^+ curve.

This situation changes dramatically, as can be seen in Figure 5 as soon as the same experiment is conducted with a concentration of TBA^+ that is only two times higher (Figure 5a) or equals (Figure 5b) that of DB18C6. It is worth noting that while the initial value of $\Delta_o^w\varphi$ was the same as in the previous experiment ($C^o_{TBA^+}/C^w_{TBA^+} = 1$) the nominal concentration of TBA^+ was only slightly larger than that of DB18C8. It is evident (Figure 5) that the feedback curves are no longer diffusion-controlled, suggesting that $\Delta_o^w\varphi$ changed dramatically as the micropipet approached the DCE/W interface. Hence, it is conceivable that the depletion and accumulation of TBA^+ in the aqueous and organic sides of the interface, respectively, which are due to IT compensation, cause $\Delta_o^w\varphi$ to shift to substantially more positive values. The positive shift of $\Delta_o^w\varphi$ causes K^+ transfer to slow, resulting in a much less pronounced feedback. Parts c and d of Figure 6 show that when the concentration of TBA^+ is equal to that of DB18C6, $\Delta_o^w\varphi_{mix}$ becomes highly dependent on L. On one hand, at long distances ($L = 2$) the regeneration of DB18C6 is diffusion-controlled, which is in agreement with experimental results (Figure 5). On the other hand, at short distances ($L = 0.1$), the mass transfer of K^+ to the DCE/W interface is enhanced to such an extent that the rate of TBA^+ transfer can no longer cope with it, causing $\Delta_o^w\varphi_{mix}$ to shift to more positive values. In fact, $\Delta_o^w\varphi_{mix}$ is shifted to a value at which the rate of TBA^+ transfer is diffusion-controlled while that of DB18C6 regeneration is very small, which is in agreement with Figure 5.

The model predicts that, under the above experimental conditions, all feedback curves should be diffusion-controlled at $L = 2$. Figure 5 shows that this is indeed the case. The model also predicts that, at $L = 0.1$, the feedback current at the micropipet should be proportional to $i^{l,w}_{TBA^+}$, the diffusion-controlled current of TBA^+ from the aqueous phase to the active area on the interface. The calculated collection efficiency, i.e., the ratio between the currents at the micropipet tip and at the lower interface, equals 1, for $L = 0.1$. This essentially implies that the feedback current (on the micropipet) must equal $i^{l,w}_{TBA^+}$. By simulations we have found that $\gamma = 1.34$ when $L = 0.1$. The expected feedback currents (at $L = 0.1$) when the ratio $C^w_{TBA^+}/C^o_{DB18C6}$ equals 1 and 2 should therefore be 1.34 and 2.68, respectively. The measured currents are 1.35 and 2.47, in good agreement with the expected values.

It can be concluded that, as long as the concentration of the potential-determining/compensating ions is small relative to the concentration of the charge carriers across the interface, mass-

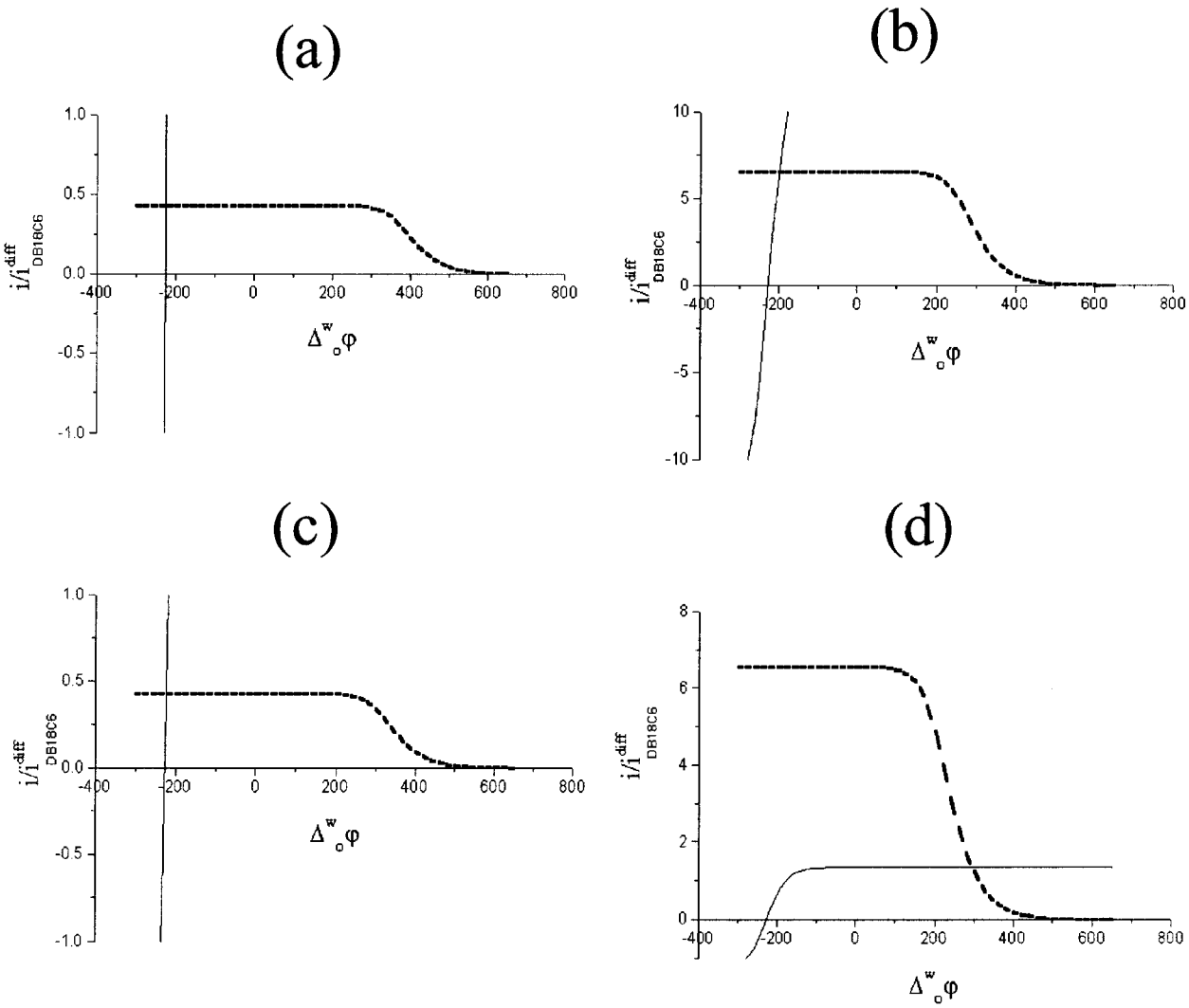

Figure 6. The model: calculated $i-\Delta^{w}_{o}\varphi$ curves for TBA^+ (—) and $K^+DB18C6$ (- - -) at the DCE/W interface. (a) $L = 2$, $C^{w}_{TBA^+} = C^{o}_{TBA^+} \gg C^{o}_{DB18C6}$. (b) $L = 0.1$, $C^{w}_{TBA^+} = C^{o}_{TBA^+} \gg C^{o}_{DB18C6}$. (c) $L = 2$, $C^{w}_{TBA^+} = C^{o}_{TBA^+} = C^{o}_{DB18C6}$; (d) $L = 0.1$, $C^{w}_{TBA^+} = C^{o}_{TBA^+} = C^{o}_{DB18C6}$.

transfer limitations of the above ions dictate the overall kinetics of the charge-transfer process.

This behavior has actually been observed in the past, in several SECM studies. Bard and Mirkin[10] were the first to apply the SECM for studying charge-transfer processes at liquid/liquid interfaces. Their first study focused on ET between ferrocene species in nitrobenzene and other redox species in an aqueous phase. IT limitations on the overall kinetics due to IT−ET coupling were observed in this study on two occasions. When the organic phase did not contain electrolyte, ET into the aqueous phase was accompanied by the transfer of ferrocenium in the same direction. A coarse treatment for this coupling has been given. In another system the effect of the concentration of tetraethylammonium (TEA^+), which served as the potential-determining ion, on the shape of feedback curves was examined. A set of approach curves was measured for a constant potential across the interface, using the same concentrations of TEA^+ on both sides, however with different ratios relative to that of the oxidizing species in the aqueous phase. IT of TEA^+ into the aqueous phase maintained electroneutrality. It was observed that, as long as the concentration of TEA^+ was kept 10 times higher than the concentration of the oxidizing species, IT limitations were eliminated. On the other hand, when the concentration of TEA^+ equaled that of the oxidizing species, the effect of the IT process on the feedback curve predominated. These results are in excellent agreement with our findings. They also demonstrate the applicability of our model to other modes of coupling, such as ET−IT. First, although initially the potential across the water/nitrobenzene interfaces was the same, it clearly had been changed during the approach curves under the different conditions that were used. Otherwise all the feedback curves would have overlapped, because ET processes should be identical for a given potential across the interface. Second, compensating IT processes are not likely to occur across the whole interface, but rather across a limited area under the SECM tip. Otherwise no IT limitations would have been expected for TEA^+/oxidizer concentration ratios ≤ 1.

A reverse electron transfer, in which an electron was transferred uphill from a redox couple with a higher standard reduction potential in one phase to another redox couple having a lower standard reduction potential in a second immiscible phase, was demonstrated by Bard.[11] The driving force for the reverse ET was the presence of an appropriate potential-determining ion that governed the interfacial potential difference. The redox species were TCNQ and ferrocyanide in the organic and aqueous phases, respectively. The potential-determining ion was tetraphenylarsonium ($TPAs^+$). The driving force that was supplied by this ion is expected to give a much more pronounced feedback[10] than that which had been reported. It is our understanding of this system that $TPAs^+$ poses two different

IT limitations. As a result of the compensating transfer, $TPAs^+$ was depleted from the aqueous side and accumulated at the organic side. As a consequence, the initial driving force decreased continuously during the approach curve. Moreover, because it is our assumption that compensating transfer takes place only under the SECM tip, the diffusion of $TPAs^+$ to the interface became effectively more hindered as the tip approached the interface.

Mirkin[17] also observed IT limitations in his paper where he first introduced the system that is the subject of this paper. The effect on the feedback was less pronounced, though, and it occurred with a smaller $C^{w}_{TBA^+}/C^{o}_{DB18C6}$ ratio on the order of 0.4. This is not surprising taking into account the fact that the micropipets that were used in that study exhibited a hemispherical-type behavior. Mirkin's observation can be justified by the following approximate treatment: The collection efficiency of a hemispherical microelectrode at $L = 0.1$ is roughly 1. The calculated diffusion-controlled current for such an electrode at this distance is ~ 3.[27,34] At the same time, the corresponding current at a disk-shaped microelectrode is ~ 8. The flux of ions to the interface is smaller when the electrode has a spherical shape.[27] This means that under such conditions the compensating ions have to cope with a substantial lower rate of charge transfer to keep electroneutrality. IT limitations are therefore expected to begin at a concentration ratio of $\sim 3/8 = 0.375$, which is in agreement with Mirkin's observation.

Conclusions

Processes of CTC across interfaces are general phenomena. Yet, they usually take place in extremely complicated biological systems that prohibit their quantitative understanding. In this paper we proposed an approach based on the SECM which could be used to induce and probe coupling between two ion-transfer processes across a simple interface between two immiscible liquid phases. The results were analyzed using a simple model that is applicable under steady-state conditions. Both the experimental method and the model are general, and can be used with other modes of coupling as well as other interfaces. The simplicity of the system makes it possible to analyze separately the different contributions, i.e., charge-transfer kinetics and mass-transfer limitations, to the overall process. The results demonstrate the pronounced effect that mass-transfer limitations of the coupled processes are likely to pose on the potential across the interface. Work in our group is in progress to elaborate the above model to a full comprehensive treatment of coupling and to apply the above experimental method to investigate other coupling processes as well as systems with biological relevance.

Acknowledgment. This research was supported by the Foundation for Basic Research administrated by the Israel Academy of Sciences and Humanities (Grant 597/97-1) and the Israeli Ministry of Science (Grant 8931).

Appendix

The concentrations in the following refer to values at the DCE/W interface unless stated otherwise.

The reaction at the DCE/W interface is

$$K^+DB18C6(o) \leftrightarrow K^+(w) + DB18C6(o) \quad (a)$$

It can be divided into two steps:

$$K^+DB18C6(o) \leftrightarrow K^+(o) + DB18C6(o) \quad (b)$$

$$K^+(o) \leftrightarrow K^+(w) \quad (c)$$

These two steps are arbitrary; the final result is general regardless of the exact mechanism of IT.[35] The equilibrium constant in the organic phase is

$$K^0 = \frac{C^{o}_{K^+} C^{o}_{DB18C6}}{C^{o}_{K^+DB18C6}} \quad (d)$$

Under reversible conditions, the Nernst−Donnan equation for the overall process is

$$\Delta^{w}_{o}\varphi = \Delta^{w}_{o}\varphi^{0}_{K^+DB18C6} - \frac{RT}{zF}\ln\frac{C^{w}_{K^+} C^{o}_{DB18C6}}{C^{o}_{K^+DB18C6}} \quad (e)$$

For the IT of K^+ the equation is

$$\Delta^{w}_{o}\varphi = \Delta^{w}_{o}\varphi^{0}_{K^+} - \frac{RT}{zF}\ln\frac{C^{w}_{K^+}}{C^{o}_{K^+}} \quad (f)$$

It is easy to see that

$$\Delta^{w}_{o}\varphi = \Delta^{w}_{o}\varphi^{0}_{K^+} + \frac{RT}{zF}\ln K^0 - \frac{RT}{zF}\ln\frac{C^{w}_{K^+} C^{o}_{DB18C6}}{C^{o}_{K^+DB18C6}} \quad (g)$$

Under steady-state conditions, the currents of all species to the interface must be equal:

$$i = nFAm^{w}_{K^+}C^{w}_{K^+} = nFAm^{o}_{DB18C6}C^{o}_{DB18C6} = nFAm^{o}_{K^+D18C6}(C^{*o}_{K^+D18C6} - C^{o}_{K^+D18C6}) \quad (h)$$

where m is the mass-transfer coefficient of the different species. $C^{*o}_{K^+DB18C6}$ is the bulk value of the ion−ionophore complex.

i_l is the diffusion-controlled current of the ion−ionophore complex to the DCE/W interface, and it is defined as

$$i_l = nFAm^{o}_{K^+DB18C6}C^{*o}_{K^+DB18C6} \quad (i)$$

Under the SECM configuration, because the extraction of K^+ out of the micropipet is diffusion-controlled, $C^{o*}_{K^+DB18C6}$ is essentially C^{o*}_{DB18C6}.

Using eq g−i, we obtain

$$\Delta^{w}_{o}\varphi = \Delta^{w}_{o}\varphi^{0}_{K^+} + \frac{RT}{zF}\ln K^0 + \frac{RT}{zF}\ln(nFAm^{w}_{K^+}) + \frac{RT}{zF}\ln\frac{i^2}{i_l - i} \quad (j)$$

Considering the fact that K^+ is diffusing away from a circular source on the interface into the bulk, the term $nFAm^{w}_{K_+}$ can be substituted with $4nFD^{w}_{K_+}\gamma a$.

References and Notes

(1) Nicholls, D. G.; Ferguson, S. G. *Bioenergetics 2*; Academic Press: London, 1992.
(2) Kakiuchi, K. *Electrochim. Acta* **1995**, *40*, 2999.
(3) Cunnane, V. J.; Schiffrin, D. J.; Beltran, C.; Geblewicz, G.; Solomon, T. *J. Electroanal. Chem.* **1988**, *247*, 203.
(4) Maeda, K.; Kihara, S.; Suzuki, M.; Matsui, M. *J. Electroanal. Chem.* **1991**, *303*, 171.
(5) Volkov, A. G.; Gugeshashvili, M. I.; Deamer, D. W. *Electrochim. Acta* **1995**, *40*, 2859.
(6) Volkov, A. G. *Electrochim. Acta* **1998**, *44*, 139.
(7) Girault, H. H.; Schiffrin, D. J. In *Electroanalytical Chemistry*; Bard A. J., Ed.; Marcel Dekker: New York, 1989; Vol. 15, p 1.

(8) Girault, H. H. In *Modern Aspects of Electrochemistry*; Bockris, J. O., Conway B. E., White R. E., Eds.; Plenum Press: New York, 1993; p 1.
(9) Samec, Z.; Kakiuchi, T. In *Advances in Electrochemical Science and Engineering*; Gerischer, H., Tobias C. W., Eds.; VCH: Weinheim, 1990; Vol. 4, p 297.
(10) Wei, C.; Bard, A. J.; Mirkin, M. V. *J. Phys. Chem*. **1995**, *99*, 16033.
(11) Solomons, T.; Bard, A. J. *J. Phys. Chem*. **1995**, *99*, 17487.
(12) Tsionsky, M.; Bard, A. J.; Mirkin, M. V. *J. Phys. Chem*. **1996**, *100*, 17881.
(13) Tsionsky, M.; Bard, A. J.; Mirkin, M. V. *J. Am. Chem. Soc*. **1997**, *119*, 10785.
(14) Shao, Y., Mirkin, M. V.; Rusling, *J. F. J. Phys. Chem*. **1997**, *101*, 3202.
(15) Shao, Y.; Mirkin, M. V. *J. Phys. Chem. B* **1998**, *102*, 9915.
(16) Barker, A. L.; Macpherson, J. V.; Slevin, C. J.; Unwin, P. R. *J. Phys. Chem. B* **1998**, *102*, 1586.
(17) Shao, Y.; Mirkin, M. V. *J. Electroanal. Chem*. **1997**, *439*, 137.
(18) Shao, Y.; Osborne, M. D.; Girault, H. H. *J. Electroanal. Chem*. **1991**, *318*, 101.
(19) Beattie, P. D.; Delay, A.; Girault, H. H. *J. Electroanal. Chem*. **1995**, *380*, 167.
(20) Samec, Z.; Papoff, P. *Anal. Chem*. **1990**, *62*, 1010.
(21) Shao, Y.; Mirkin, M. V. *J. Am. Chem. Soc*. **1997**, *119*, 8103.
(22) Shao, Y.; Liu, B.; Mirkin, M. V. *J. Am. Chem. Soc*. **1998**, *120*, 12700.
(23) Selzer, Y.; Turyan, I.; Mandler, D. *J. Phys. Chem. B* **1999**, *103*, 1509.
(24) Shao, Y.; Mirkin, M. V. *Anal. Chem*. **1998**, *70*, 3155.
(25) Bard, A. J.; Mirkin, M. V.; Unwin, P. R.; Wipf, D. O. *J. Phys. Chem*. **1992**, *96*, 1861.
(26) Macpherson, J. V.; Unwin, P. R. *J. Phys. Chem*. **1994**, *98*, 1704.
(27) Selzer, Y.; Mandler, D. Submitted for publication.
(28) Bard, A. J.; Faulker, L. R. *Electrochemical Methods*; Wiley: New York, 1980.
(29) Samec, Z. *J. Electroanal. Chem*. **1979**, *103*, 1.
(30) Unwin, P. R. *J. Chem. Soc., Faraday. Trans.* **1998**, *94*, 3183.
(31) Amphlett, J. L.; Denuault, G. *J. Phys. Chem. B* **1998**, *102*, 9946.
(32) Stewart, A. A.; Taylor, G.; Girault, H. H.; McAleer, J. *J. Electroanal. Chem*. **1990**, *296*, 491.
(33) Mirkin, M. V.; Bard, A. J. *Anal. Chem*. **1992**, *64*, 2293.
(34) Mirkin, M. V.; Fan, F.-R. F.; Bard, A. J. *J. Electroanal. Chem*. **1992**, *328*, 47.
(35) Matsuda, H.; Yamada, Y.; Kanamori, K.; Kudo, Y.; Takeda, *Y. Bull. Chem. Soc. Jpn*. **1991**, *64*, 1497.